Computational Study about Through-Bond and Through-Space Interactions in [2.2]Cyclophanes

Giovanni F. Caramori and Sérgio E. Galembeck*

Departamento de Química, Faculdade de Filosofia, Ciencias e Letras de Ribeirão Preto, Universidade de São Paulo, 14040-901, Ribeirão Preto − SP, Brazil

Received: October 19, 2006

An analysis of the electron density, obtained by B3PW91/6-31+G(d,p), B3LYP/6-31+G(d,p), and MP2/6-31+G(d,p) for [2,2]cyclophanes isomers, [2.2]paracyclophane, *anti*-[2.2]metacyclophane, *syn*-[2.2]metacyclophane, and [2.2]metaparacyclophane, was made through natural bond orbitals (NBO), natural steric analysis (NSA), and atoms in molecules (AIM) methods and through analysis of frontier molecular orbitals (MOs). NBO indicates that all compounds present through-bond interactions, but only the conformers of [2.2]-metacyclophane present significant through-space interactions. The last interactions are observed in AIM analysis and by the plots of MOs. AIM indicates that these through-space interactions are closed-shell ones, and they stabilize the conformers. In contrast, all isomers present through-bond and through-space repulsive interactions. In addition, the atomic properties, computed over the atomic basins, showed that the position of the bridges and the relative displacement of the rings can affect the atomic charges, the first atomic moments, and the atomic volumes.

1. Introduction

The [2.2]cyclophanes are the simplest [2$_n$]cyclophanes that present two phenyl rings connected by two ethanediyl linkages.[1] They are classified according to the location of the $-CH_2CH_2-$ linkage and the orientation of the benzene rings (anti and syn) such as [2.2]paracyclophane, (**1**); *anti*-[2.2]metacyclophane, (**2a**); *syn*-[2.2]metacyclophane, (**2b**); and [2.2]metaparacyclophane, (**3**) (Figure 1). The structural characteristics of these compounds make possible to investigate the presence of the $\pi-\pi$ transannular interaction and its influence on the chemical properties.[2]

Since the pioneering studies performed by Cram and coworkers,[3] the chemistry of cyclophanes has presented a large development and it has also attracted considerable interest of chemists. Nowadays, the cyclophanes have shown several important applications, such as auxiliary in asymmetric synthesis[4] and catalysts that simulate enzymatic functions, presenting selectivity in relation to the substrates.[5] The cyclophanes have applications not only in different synthetic processes but also in supramolecular chemistry[6] and in the biomedical areas.[7] Polymers prepared from cyclophanes by chemical deposition on vapor phase (CVD)[8] can compose biomimetical layers with incorporated functional groups (proteins, antigens, cell receptors) which allow the control of the interactions between biomaterials and the organisms.[7] These compounds also act as selective synthetic receptors of anions that exhibit biological function, for example, carboxylates and phosphates.[9] Cyclophanes and their derivatives are also used as a model to investigate the host−guest hydrophobic association in water.[11]

Studies using photoelectron spectroscopy and electron spin resonance (ESR) have shown that [2.2]paracyclophane and its derivatives can present transannular interactions that stem from direct interaction of orbitals by the space (through-space) or through chemical bonds (through-bond).[13] The transannular interactions and the chemical properties of [2.2]cyclophanes are directly related with the proximity between the aromatic rings (Figure 1).[2] Transannular interactions have presented an important role in the cyclophane chemistry. They are used to explain the behavior of several reactions. For example, the different formylation behaviors of [2.2]metacyclophanes can be explained by the extra stability of cationic intermediates, which stem from through-space interactions between the benzene rings.[14] An analogous explanation was also attributed to the acylation of 8,16-disubstituted [2.2]metacyclophanes.[15] Fedyanin et al., through the atoms in molecules (AIM) analysis, have also shown that though-space interactions promote the stabilization of [2.2]paracyclophane radical anions.[16] In addition, nonlinear optical properties such as β quadratic hyperpolarizability have provided strong evidence of significant through-space interactions in [2.2]paracyclophane derivatives.[17,18] Furthermore, some recent computational studies that consider atoms in molecules theory have demonstrated that cation$-\pi$ complexes of substituted [*n*.*n*]paracyclophanes (n = 2, 3) present strong through-space interactions, induced by the substituents, which affect the binding energy between the cation and the nonsubstituted ring.[19] In addition, the AIM analysis has been employed as a reliable tool to investigate the ion$-\pi$ interactions in [*n*,*n*]paracyclophanes.[20,21]

Therefore, a computational study that investigates the transannular interactions can provide an essential insight into the way in which the cyclophane rings communicate with one another and how much stabilization arises from these interactions. In this sense, the purpose of this work is to analyze mechanisms (through-space or through-bond) of the transannular interactions in the [2.2]cyclophanes isomers, **1**−**3**, by using AIM and atoms in molecules (NBO) methods. In a first paper, a study was made about the best model to describe the conformations, the stability, the aromaticity, the charges, and the chemical shifts of these compounds.[22]

* Author to whom correspondence should be addresed. E-mail: segalemb@usp.br.

10.1021/jp066863h CCC: $37.00
Published on Web 02/13/2007

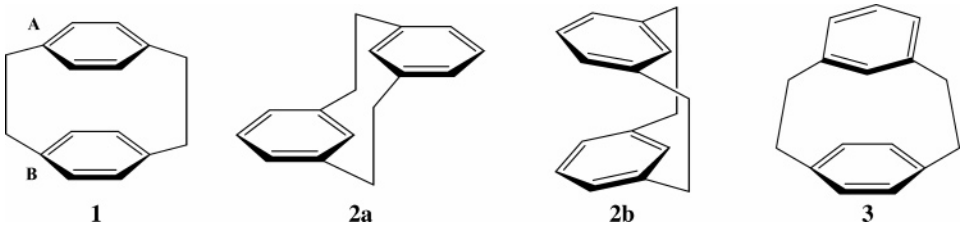

Figure 1. [2.2]Cyclophanes.

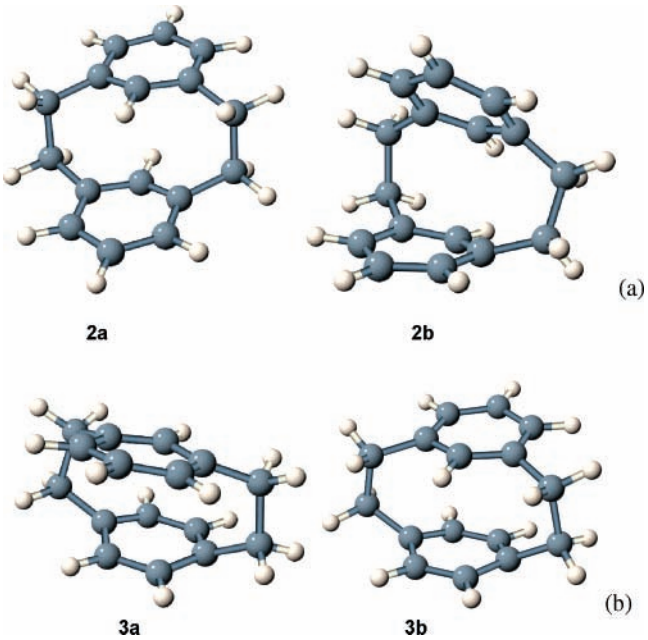

Figure 2. (a) Conformers of [2.2]metacyclophanes, (b) degenerated conformers of [2.2]metaparacyclophane.

2. Computational Methods

The geometries were optimized by B3PW91[23]/6-31+G(d,p),[24] B3LYP[25]/6-31+G(d,p), and MP2[26]/6-31+G(d,p) as reported in a previous paper,[22] and the vibrational frequencies were calculated by the first two models to verify that all isomers are minima in the potential energy surface. Electron densities were obtained by B3PW91/6-31+G(d,p) and B3LYP/6-31+G(d,p), with Gaussian98 software.[27] As the results for both models are similar, only results for the first are presented. The electronic structure was investigated with NBO,[28] natural steric analysis (NSA),[29] and AIM[30] methods. In addition, the plot of the frontier orbitals was analyzed to verify the possibility of occurrence of transannular interactions. The resonance structures of the isomers were investigated with the NRT[31] method. The NBO, NSA, and NRT analyses were carried out with the NBO 5.0 program.[32] Morphy98[33] and AIM2000[34] programs were used for the AIM analysis from MP2/6-31+G(d,p) calculations. The molecular orbitals (MOs) were visualized by using Molekel 4.3.[35] The NBOs and NLMOs were visualized with NBOView 1.0.[36]

3. Results and Discussion

3.1. Considerations about Geometry. According to our previous results,[22] [2.2]paracyclophane, **1**, presents only a rigid structure but the methylene bridges can show small distortions from the parallelism to relief steric repulsions, reducing the point group from D_{2h} to D_2. For several years, these distortions have been a matter of debate between structural chemists. An eight-year-old article indicates that **1** presents D_2 point group.[37] Two different conformers of [2.2]metacyclophane, **2**, were obtained, *anti*[2.2]metacyclophane, **2a**, the most stable, and *syn*[2.2]-metacyclophane, **2b** (Figure 2a). The small stability of the latter can be attributed to the repulsive interaction between aromatic clouds, stacking (Figure 1). The isomer **3** presents two degenerate conformers, **3a** and **3b**. According to these results, there are two conformers **2a** and **2b** for the isomer **2** and a unique conformer **3a** for the isomer **3** (Figure 2b). Additional calculations (geometry optimizations and vibrational frequencies) employing the model B3PW91/6-311++G(d,p) were computed to the conformers **2a** and **2b**. The results were compared with those obtained by using the model B3PW91/6-31+G(d,p), indicating that the differences on the geometries superposition and energies present standard deviations less than 1.0×10^{-3}, indicating the reliability to the results reported in this manuscript.

TABLE 1: The Main Resonance Structures of 1−3a, Considered in the NBO and NSA Analysis (B3PW/6-31+G(d,p))

Compounds	Resonance structures	
1	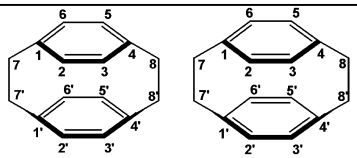 **1A**	**1A'**
2a	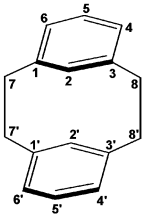 **2A**	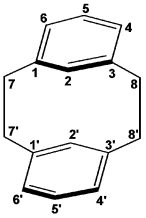 **2A'**
2b	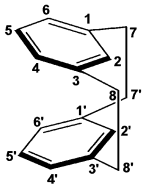 **2B**	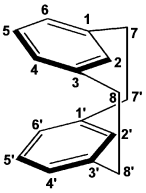 **2B'**
3a	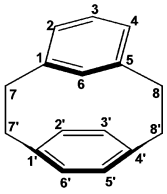 **3A**	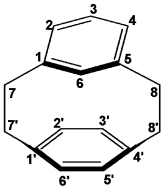 **3A'**

3.2. Attractive Interactions between Natural Bond Orbitals. The NBO analysis was applied to the main resonance structure, RS, of **1**−**3a** (**1A**−**3A′**) (Table 1), which were obtained through the NRT method.[31] The second-order stabilization energies, reported in this manuscript, were determined by

TABLE 2: Second-Order Stabilization Energy ($\Delta E^{(2)}$) for the Main Resonance Structures of the [2.2]Cyclophanes Isomers (B3PW91/6-31+G(d,p))

	ΔE^2 (kcal/mol)							
interactions	**1A**	**1A′**	**2A**	**2A′**	**2B**	**2B′**	**3A**	**3A′**
$\pi_{C(1)-C(6)} \rightarrow \pi^*_{C(2)-C(3)}$	19.05	19.05	18.62	18.50	18.82	21.05	19.65	19.65
$\pi_{C(1)-C(6)} \rightarrow \pi^*_{C(4)-C(5)}$	21.87	21.87	21.55	21.48	21.13	18.68	22.11	22.11
$\pi_{C(1)-C(6)} \rightarrow \sigma^*_{C(7)-C(7')}$			3.11	3.13	3.34	3.35	3.89	3.89
$\pi_{C(1')-C(2')} \rightarrow \pi^*_{C(2)-C(3)}$		0.61		1.87		2.35		
$\pi_{C(1')-C(2')} \rightarrow \pi^*_{C(3')-C(4')}$		21.87		21.08		21.77		21.54
$\pi_{C(1')-C(2')} \rightarrow \pi^*_{C(5')-C(6')}$		19.06		19.95		19.06		17.86
$\pi_{C(1')-C(2')} \rightarrow \sigma^*_{C(7)-C(7')}$				3.53		3.90		
$\pi_{C(1')-C(6')} \rightarrow \pi^*_{C(2')-C(3')}$	19.03		18.64		18.84		19.46	
$\pi_{C(1')-C(6')} \rightarrow \sigma^*_{C(7)-C(7')}$					3.36		3.80	
$\pi_{C(2)-C(3)} \rightarrow \pi^*_{C(1')-C(2')}$		0.61		1.87		2.35		
$\pi_{C(2)-C(3)} \rightarrow \sigma^*_{C(8)-C(8')}$			3.52	3.53	3.90	3.89		
$\pi_{C(2)-C(3)} \rightarrow \pi^*_{C(4)-C(5)}$	19.08	19.08	19.98	19.95	19.09	19.06	18.85	18.85
$\pi_{C(2')-C(3')} \rightarrow \pi^*_{C(1')-C(6')}$	19.08		21.13		21.77		18.57	
$\pi_{C(2')-C(3')} \rightarrow \sigma^*_{C(8)-C(8')}$					2.64			
$\pi_{C(3')-C(4')} \rightarrow \pi^*_{C(1')-C(2')}$		21.58		18.51		21.06		21.54
$\pi_{C(3')-C(4')} \rightarrow \sigma^*_{C(8)-C(8')}$		3.12		3.13		3.34		2.91
$\pi_{C(4)-C(5)} \rightarrow \pi^*_{C(1)-C(6)}$	21.58	21.58	18.96	18.91	19.61	19.91	18.26	18.26
$\pi_{C(4)-C(5)} \rightarrow \sigma^*_{C(8)-C(8')}$							3.17	3.17
$\pi_{C(4')-C(5')} \rightarrow \pi^*_{C(1')-C(6')}$	21.87		18.97		18.82		22.36	
$\pi_{C(4')-C(5')} \rightarrow \sigma^*_{C(8)-C(8')}$							3.80	
$\pi_{C(5')-C(6')} \rightarrow \pi^*_{C(1')-C(2')}$		18.85		19.85		19.93		19.35
$\sigma_{C(7)-C(7')} \rightarrow \pi^*_{C(1)-C(6)}$	3.41	3.41	4.30	4.18	2.80	2.81	3.38	3.38
$\sigma_{C(8)-C(8')} \rightarrow \pi^*_{C(2)-C(3)}$			4.10	4.06		3.83		
$\sigma_{C(8)-C(8')} \rightarrow \pi^*_{C(3')-C(4')}$				4.19		2.80		4.58

using the B3PW91/6-31+G(d,p) electron densities because the NBO method evaluates these energies only when there is a well-defined one-electron effective Hamiltonian operator (Fock or Kohn−Sham operator). In relation to the RS **1A**, **2A**, **2B**, and **3A**, the main interactions that can be observed are $\pi \rightarrow \pi^*$, involving orbitals localized in the same ring. These interactions are around 20.0 kcal mol^{-1} and contribute to the stabilization of these structures. Some through-bond interactions were observed between π orbitals of rings and σ^* orbitals of ethano-bridges and between σ orbitals of ethano-bridges and π^* orbitals of rings. For example, **1A** presents only one through-bond interaction $\sigma \rightarrow \pi^*$ which provides a stabilization around 3.0 kcal mol^{-1}. In addition, the structures **2A**, **2B**, and **3A** present more than one through-bond interaction, which provides stabilizations around 3−4 kcal mol^{-1}. The through-space interactions ($\pi \rightarrow \pi^*$, involving orbitals localized in different rings), were not observed for these RS.

With regard to **1A′**, **2A′**, **2B′**, and **3A′**, the behavior of the interactions is very similar with that observed for a first set of RS. The interactions that provide more stabilization (around 20 kcal mol^{-1}) are those that occur between π and π^* orbitals in the same aromatic ring (Table 2). The magnitude of the through-bond interactions is similar for both groups of resonance structures. The number of through-bond interactions is larger for **1A**−**3A** than for **1A′**−**3A′**, which suggests that the last group of RS is less stabilized by these interactions than the first one. The through-space interactions were observed only for **1A′**, **2A′**, and **2B′**, with stabilizations of 0.61, 1.87, and 2.35 kcal mol^{-1}, respectively. According to the second-order energetic analysis, for all RS, the number of the through-space interactions is lower than the number of the through-bond interactions, and the last are not so stabilized. These results imply that the isomers of

TABLE 3: Second-Order Stabilization Energy, $\Delta E^{(2)}$, in kcal mol^{-1}, Energy Difference between Donor and Acceptor Orbitals, ϵ(i) − ϵ(j), and Fock Matrix Elements, F(i,j), in Hartree, (B3PW91/6-31+G(d,p))

interactions	RS	$\Delta E^{(2)}$	ϵ(i) − ϵ(j)	F(i,j)
$\pi_{C(1)-C(6)} \rightarrow \pi^*_{C(4)-C(5)}$	**2B′**	18.68	0.28	0.065
	3A	22.11	0.28	0.070
$\pi_{C(1)}$-C(6) $\rightarrow \sigma^*_{C(7)}$-C(7′)	**2A**	3.11	0.59	0.042
	2B	3.34	0.58	0.044
	3A	3.89	0.58	0.046
$\pi_{C(2)}$-C(3) $\rightarrow \pi^*_{C(1')}$-C(2′)	**1A′**	0.61	0.28	0.012
	2A′	1.87	0.28	0.021
	2B′	2.35	0.28	0.023
$\sigma_{C(7)}$-C(7′) $\rightarrow \pi^*_{C(1)}$-C(6)	**1A′**	3.41	0.60	0.044
	2A	4.30	0.61	0.050
	2B	2.80	0.61	0.040

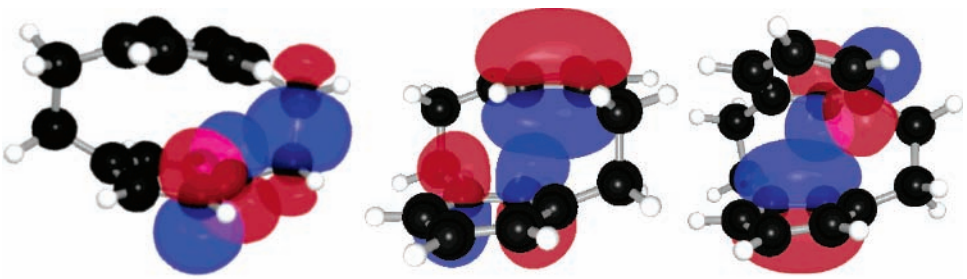

Figure 3. Through-bond and through-space interactions between NBOs.

TABLE 4: Occupations of NBOs of the Main RS of 2a and 2b, Obtained by Using the Models B3PW91/6-31+G(d,p) and MP2/6-31+G(d,p)

	Occupations							
NBOs	B3PW91/6-31+G(d,p)				MP2/6-31+G(d,p)			
	2A	**2A′**	**2B**	**2B′**	**2A**	**2A′**	**2B**	**2B′**
$\pi_{C(1')-C(2')}$		1.6579		1.6478		1.5810		1.5988
$\pi_{C(1)-C(6)}$	1.6312	1.6281	1.6581	1.6585	1.6075	1.6070	1.6077	1.6080
$\pi_{C(1')-C(6')}$	1.6434		1.6512		1.6075		1.5999	
$\pi_{C(2)-C(3)}$	1.1192	1.6579	1.6473	1.9737	1.5815	1.5807	1.5983	1.5989
$\pi_{C(2')-C(3')}$	1.3065		1.6364		1.5815		1.5872	
$\pi_{C(3')-C(4')}$		1.6281		1.6584		1.6070		1.6080
$\pi_{C(4)-C(5)}$	1.4125	1.6769	1.6772	1.6774	1.6270	1.6269	1.6279	1.6280
$\pi_{C(4')-C(5')}$	1.4074		1.6636		1.6270		1.6139	
$\pi_{C(5')-C(6')}$		1.6768		1.6774		1.6269		1.6280
$\sigma_{C(7)-C(7')}$	1.9464	1.9526	1.9598	1.9598	1.9198	1.9198	1.9258	1.9258
$\sigma_{C(8)-C(8')}$	1.9464	1.9526	1.9598	1.9598	1.9198	1.9198	1.9259	1.9259
$\pi^*_{C(1')-C(2')}$		0.3561		0.3454		0.3743		0.3730
$\pi^*_{C(1')-C(6')}$	0.1971		0.3601		0.3844		0.3898	
$\pi^*_{C(1)-C(6)}$	0.1619	0.3462	0.3460	0.3460	0.3844	0.3844	0.3750	0.3750
$\pi^*_{C(2)-C(3)}$	0.3159	0.3561	0.3448	0.3453	0.3749	0.3743	0.3724	0.3729
$\pi^*_{C(2')-C(3')}$	0.3809		0.3514		0.3749		0.3795	
$\pi^*_{C(3')-C(4')}$		0.3462		0.3460		0.3844		0.3760
$\pi^*_{C(4)-C(5)}$	0.2782	0.3463	0.3355	0.3354	0.3716	0.3717	0.3619	0.3618
$\pi^*_{C(4')-C(5')}$	0.2637		0.3462		0.3716		0.3729	
$\pi^*_{C(5')-C(6')}$		0.3463		0.3356		0.3717		0.3620
$\sigma^*_{C(7)-C(7')}$	0.0149	0.0252	0.0259	0.0259	0.0478	0.0478	0.0490	0.0490
$\sigma^*_{C(8)-C(8')}$	0.0149	0.0252	0.0259	0.0259	0.0478	0.0478	0.0490	0.0490

TABLE 5: Natural Steric Analysis for the Main Resonance Structures of the [2.2]Cyclophanes Isomers (B3PW91/6-31+G(d,p))

	d*E*(kcal/mol)							
NLMO(i) ↔ NLMO(j)	**1A**	**1A′**	**2A**	**2A′**	**2B**	**2B′**	**3A**	**3A′**
$\pi_{C(1)-C(2)} \leftrightarrow \pi_{C(1')-C(2')}$						2.88		
$\pi_{C(1)-C(6)} \leftrightarrow \pi_{C(2)-C(3)}$	9.10	9.10	9.39	9.48	9.02	9.79	9.44	9.48
$\pi_{C(1)-C(6)} \leftrightarrow \pi_{C(2')-C(3')}$			1.03					
$\pi_{C(1)-C(6)} \leftrightarrow \pi_{C(4)-C(5)}$	8.03	8.04	8.59	8.57	8.69	8.44	9.13	9.13
$\pi_{C(1)-C(6)} \leftrightarrow \sigma_{C(7)-C(7')}$	8.59	8.63	8.16	7.93	8.38	5.68		
$\pi_{C(1)-C(6)} \leftrightarrow \pi_{C(1')-C(6')}$	6.75							
$\pi_{C(1')-C(6')} \leftrightarrow \sigma_{C(7)-C(7')}$			8.17		8.75		10.39	
$\pi_{C(2)-C(3)} \leftrightarrow \pi_{C(1')-C(2')}$				7.94		9.43		
$\pi_{C(2)-C(3)} \leftrightarrow \pi_{C(2')-C(3')}$	7.44		8.90		11.71			
$\pi_{C(2)-C(3)} \leftrightarrow \pi_{C(3')-C(4')}$		5.15				2.88		
$\pi_{C(2)-C(3)} \leftrightarrow \sigma_{C(8)-C(8')}$			8.72	8.23	8.86	8.76		
$\pi_{C(3')-C(4')} \leftrightarrow \sigma_{C(8)-C(8')}$		7.60		8.23		7.90		10.36
$\pi_{C(4)-C(5)} \leftrightarrow \pi_{C(4')-C(5')}$	6.75							
$\pi_{C(4)-C(5)} \leftrightarrow \pi_{C(5')-C(6')}$		5.15						
$\pi_{C(4)-C(5)} \leftrightarrow \sigma_{C(8)-C(8')}$	8.59						7.00	6.75
$\sigma_{C(7)-C(7')} \leftrightarrow \pi_{C(1')-C(2')}$		8.63		8.24		7.55		
$\sigma_{C(7)-C(7')} \leftrightarrow \pi_{C(1)-C(6)}$							7.60	7.59
$\sigma_{C(7)-C(7')} \leftrightarrow \pi_{C('1)-C(6')}$	7.64		8.72		8.42			
$\sigma_{C(8)-C(8')} \leftrightarrow \pi_{C(2')-C(3')}$			8.74	8.23	8.11			
$\sigma_{C(8)-C(8')} \leftrightarrow \pi_{C(3')-C(4')}$						5.67		

[2.2]cyclophanes are mainly stabilized by through-bond rather than by through-space interactions, probably by proximity effects (Figure 3). In addition, the results show that the delocalization of π electrons provides large stabilizations to these systems, according to the $\pi \rightarrow \pi^*$ interactions between occupied and unoccupied NBOs of a same ring, or the aromaticity is maintained in cyclophanes, as observed in a previous paper.[22]

The differences observed for $\Delta E^{(2)}$ values can be explained in terms of energy splitting between donor and acceptor orbitals, $\epsilon(i) - \epsilon(j)$, and off-diagonal NBO Fock matrix element, $F(i,j)$. According to Table 3, interactions involving π and π^* orbitals present constant values of $\epsilon(i) - \epsilon(j)$ (0.28 Hartree) and values of $F(i,j)$ that vary from 0.01 to 0.07 Hartree, indicating that the stabilization follows the orbital overlap. $\sigma \rightarrow \pi^*$ or $\pi \rightarrow \sigma^*$ interactions present similar $\epsilon(i) - \epsilon(j)$ values but the variation in $\Delta E^{(2)}$ can be attributed once more to $F(i,j)$. For the through-space interaction $\pi_{C(2)-C(3)} \rightarrow \pi^*_{C(1')-C(2')}$, the magnitude of $\Delta E^{(2)}$ is directly related to $F(i,j)$, while the $\epsilon(i) - \epsilon(j)$ values are maintained constant. Therefore, the differences in $\Delta E^{(2)}$, for through-bond or through-space interactions, can be explained by the variations in the off-diagonal NBO Fock matrix element, $F(i,j)$, which is proportional to $S(i,j)$ in qualitative molecular orbital theories.[38]

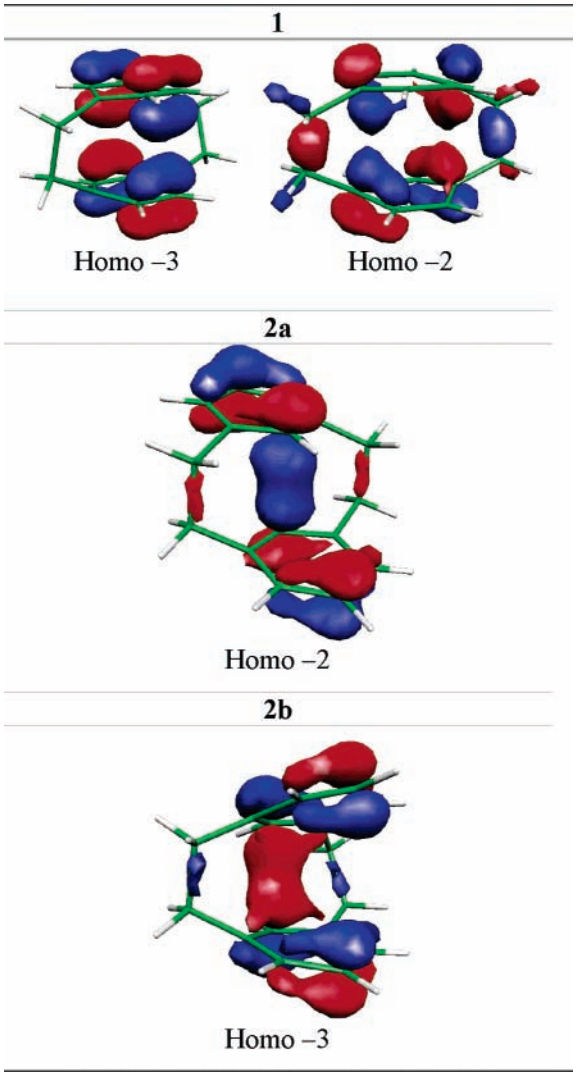

Figure 4. Frontier orbitals of the [2.2]cyclophanes.

In relation to the hybridization of the natural hybrid orbitals (NHOs), which constitute the NBOs, no changes were observed. NHOs that belong in ring or bridgehead carbons present sp^2 hybridization, while the NHOs of bridge carbons exhibit sp^3 hybridization.

To evaluate the differences of both models B3PW91/6-31+G(d,p) and MP2/6-31+G(d,p) on the NBO results, the π, π^*, σ, and σ^* orbital occupations for the RS of **2a** and **2b**, involved in the main interactions, were determined for both models. Qualitatively, the results are very similar. However, the following tendency can be observed: The occupations of the bonding orbitals are larger for B3PW91/6-31+G(d,p) than for MP2/6-31+G(d,p) model. On the other hand, an opposite behavior occurs for antibonding orbitals (Table 4), indicating that the MP2/6-31+G(d,p) model describes the electron delocalization better than B3PW91/6-31+G(d,p).

3.3. Repulsive Interactions, Natural Steric Analysis. The NSA analysis was applied to all RS, **1A**−**3A′**. The RS **1A**, **2A**, **2B**, and **3A** presented some typical steric interactions. In an analogous manner as in the NBO analysis, the local steric

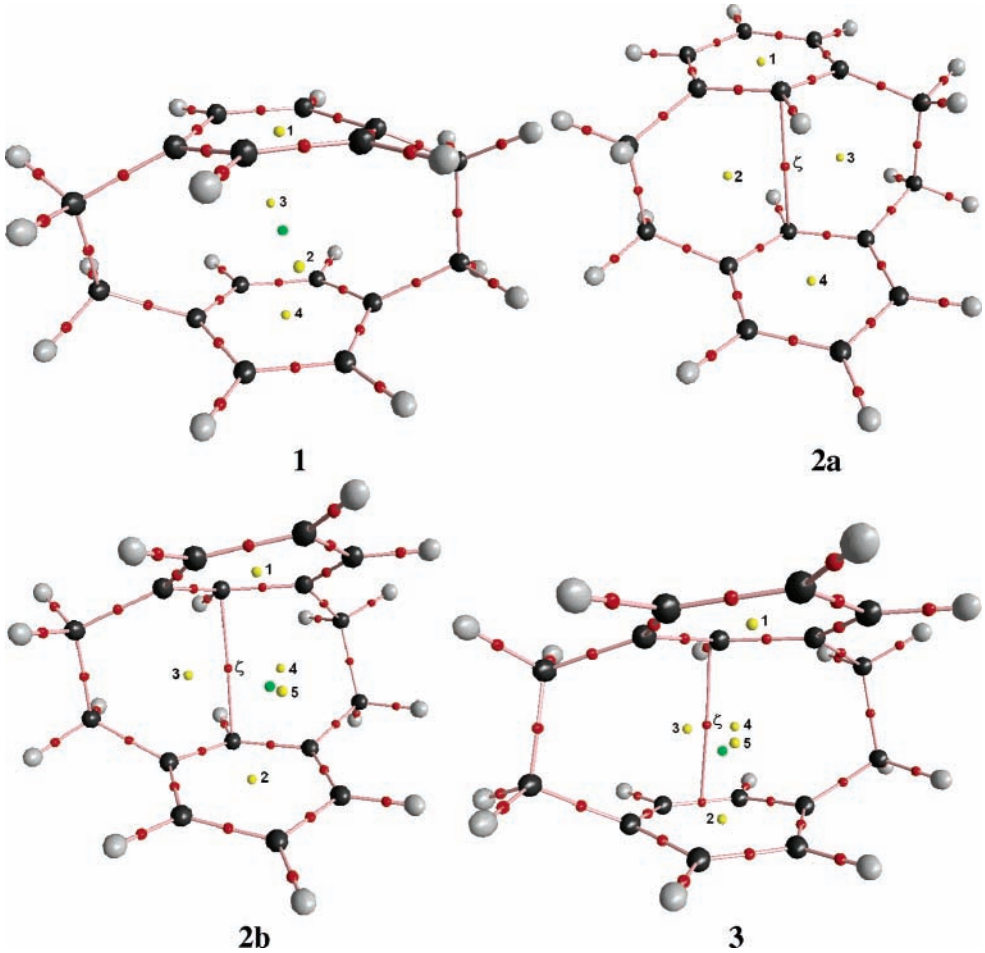

Figure 5. Molecular graphs of **1**−**3**, where the critical points (CPs) are denoted by dots and the atoms by spheres. The bond critical points (BCPs) are denoted by red dots, ring critical points (RCPs) by yellow dots, and the cage critical point (CCP) by a green dot.

repulsions between occupied NLMOs were also determined by using the B3PW91/6-31+G(d,p) electron densities. The main interactions that can be observed are those that occur between doubly occupied NLMOs of a same ring. For example, the interactions $\pi_{C(1)-C(6)} \leftrightarrows \pi_{C(2)-C(3)}$ and $\pi_{C(1)-C(6)} \leftrightarrows \pi_{C(4)-C(5)}$ are common for all structures (Table 5). The notation $\leftrightarrows$ means repulsive interaction between doubly occupied NLMOs. In addition, a large number of through-bond interactions involving π orbitals of the rings and σ orbitals of the bridges are also observed. The magnitude of these interactions ranges from 5.7 to 10.4 kcal mol^{-1}. However, more common values are around 8.0 kcal mol^{-1}, for example, $\pi_{C(1')-C(6')} \leftrightarrows \sigma_{C(7)-C(7')}$ and $\sigma_{C(7)-C(7')} \leftrightarrows \pi_{C(1')-C(6')}$. In relation to the through-space interactions involving NLMOs, all RS showed this kind of interaction, except the structures **3A** and **3A′**. In addition, the structures **1A′**, **2A′**, and **2B′** presented a very similar behavior compared to RS **1A**, **2A**, and **2B** (Table 5). Therefore, not only through-bond but also through-space interactions can occur between occupied NLMOs. These results suggest that the interactions that destabilize the cyclophanes occur by both mechanisms through-bond and through-space.

3.4. Molecular Orbitals, MOs. To investigate in detail the interaction mechanisms, the shape of the molecular orbitals MOs was analyzed. According to Salcedo et al.,[39] the shape of the MOs, mainly those around the frontier orbitals, points out the transannular effects (Figure 4).

This analysis is very useful to elucidate the probable pathways that the electrons follow when a transannular interaction occurs. Only occupied MOs from HOMO-5 present an isodensity that suggests the existence of transannular interactions by through-space mechanism. The frontier orbitals of **1**, **2a**, and **2b** show adequate shape and orientation of MO lobes for through-space interactions. In relation to the isomer **3**, there are no molecular orbitals with lobes that present an adequate orientation. These results are in good agreement with the NBO analysis, because there are no NBOs of **3** that present through-space interaction.

3.5. Topological Properties of the Electron Density, AIM. The AIM theory was applied to analyze the electron density, which was determined from the MP2/6-31+G(d,p) wave function, in all critical points of the considered cyclophanes **1**−**3**. The obtained topologies are consistent with the Poincaré-Hopf rule. Only the nonequivalent RCPs were considered in this analysis. In terms of the AIM theory, a transannular interaction can be identified by the presence of a BCP between the carbon atoms that belong in different aromatic rings, for example, C(1)···C(1′), C(2)···C(2′), C(3)···(C3′), and others.[40] Despite that fact that some authors criticize the statement that the presence of a bond critical point and a bond path is not a sufficient condition for the presence of bonding interactions,[41a−b] Bader affirms, through well-established arguments, that the presence of a bond path is a universal indicator of bonding.[42a−b]

According to the molecular graph of **1** (Figure 5), there are no BCPs between carbons of different rings, indicating that in this case, the presence of transannular interactions is not observed. Conversely, the isomers **2a** and **2b** present BCPs ζ that connect carbons from different rings, suggesting the existence of transannular interactions. These results are in close agreement with NBO and MOs analyses. In relation to the

TABLE 6: Properties of BCPs, RCPs, and CCPs (au), (MP2/6-31+G(d,p))

		compounds			
critical points	properties	**1**	**2a**	**2b**	**3**
		BCPs			
C(1)−C(2)	ρ_b	0.305	0.306	0.306	0.305
	$\nabla^2\rho_b$	−0.814	−0.817	−0.819	−0.816
	ϵ	0.205	0.208	0.204	0.205
C(1)−C(6)	ρ_b	0.306	0.305	0.306	0.306
	$\nabla^2\rho_b$	−0.819	−0.813	−0.816	−0.817
	ϵ	0.202	0.202	0.209	0.204
C(1)−C(7)	ρ_b	0.253	0.256	0.255	0.252
	$\nabla^2\rho_b$	−0.602	−0.614	−0.608	−0.599
	ϵ	0.031	0.038	0.034	0.030
C(2)−C(3)	ρ_b	0.307	0.307	0.308	0.307
	$\nabla^2\rho_b$	−0.820	−0.831	−0.830	−0.828
	ϵ	0.223	0.211	0.214	0.211
C(7)−C(7′)	ρ_b	0.217	0.225	0.219	0.224
	$\nabla^2\rho_b$	−0.444	−0.471	−0.451	−0.471
	ϵ	0.012	0.008	0.011	0.009
		RCPs			
1	ρ_b	0.021	0.021	0.021	0.021
	$\nabla^2\rho_b$	0.162	0.159	0.160	0.158
2	ρ_b	0.010	0.014		0.021
	$\nabla^2\rho_b$	0.028	0.064		0.163
3	ρ_b			0.015	0.012
	$\nabla^2\rho_b$			0.058	0.039
5	ρ_b			0.003	0.010
	$\nabla^2\rho_b$			0.009	0.034
		CCP			
	ρ_b	0.005		0.003	0.009
	$\nabla^2\rho_b$	0.019		0.011	0.036

isomer **3**, there is a BCP between the two aromatic moieties, but it is connecting two other BCPs. It means that a conflict mechanism is occurring. This conflict structure is energetically and topologically unstable, which means that a slightly conformational change will modify the distance between the aromatic rings, and therefore the BCP will vanish.[43]

According to Table 6, the electron density, ρ_b, is more localized in BCPs from CC ring bonds than in BCPs of CC bridge bonds, indicating that the concentration of electronic charge occurs preferentially in the rings. ρ_b is very similar for equivalent BCPs in different isomers, showing that the electronic density in rings or bridges is not affected by the conformational differences. On the other hand, the electronic density is reduced at RCPs, CCPs, and ζ. The Laplacian of the electron density, $\nabla^2\rho_b$, shows where the electron density is locally concentrated ($\nabla^2\rho_b < 0$) and where it is locally depleted ($\nabla^2\rho_b > 0$). It is observed that the values of $\nabla^2\rho_b$ are more negative for CC ring bonds than for CC bridge bonds. In addition, the $\nabla^2\rho_b$ is widely positive in RCPs localized at the center of aromatic rings (Figure 5, RCP 1), indicating that a large depletion in the electronic charge occurs at this position. For the other CPs, $\nabla^2\rho_b$ is approximately zero, indicating that the depletion on the electronic charge is not as intense as in the center of the rings. The ellipticity, ϵ_b, which can describe the π-character of a chemical bond, pointed out that bonds of rings exhibit an elevated π-character while the bonds of the bridges are more cylindrical, showing that the electron delocalization is restricted to the aromatic rings. In relation to the presence of transannular interactions, the AIM analysis correlates very well with the NBO results because both point out that the through-space interactions occur mainly for the isomers **2a** and **2b**, as indicated by the presence of the BCP between the carbon atoms belonging to the different aromatic rings.[40]

To characterize the transannular interactions of **2a** and **2b**, the properties of both BCPs, ζ, were analyzed and compared with those from BCPs of ordinary aromatic C−C chemical bonds, BCP_{ring}. The obtained results show that the transannular interactions of **2a** and **2b** exhibit the characteristics of closed-shell interactions[44] (Table 7): a low value of ρ_b at ζ, relatively small corresponding positive values for $\nabla^2\rho_b$, and a positive value for the energy density H_b, which is close to zero. On the other hand, covalent bonds exhibit large values of ρ_b at BCP_{ring} and negative values of $\nabla^2\rho_b$ and H_b at BCP_{ring}, indicating a shared interaction.[45] Comparing G_b and V_b, we can also note that the obtained data for ζ are smaller than for BCP_{ring}, indicating that the local kinetic and potential energy density are reduced at ζ. ϵ indicates that the curvatures of the density at ζ are very small when compared with the correspondent at BCP_{ring}. Adopting the same procedure employed by Matta et al. to investigate hydrogen−hydrogen bonds in polybenzenoids,[46] a stable transannular C−C interaction can present a large distance between BCP and RCP, $r_b - r_r$, and a large difference between the electron densities at these CPs, $\rho_b - \rho_r$. The difference between the bond path length, BPL, and the bond length, BL, needs to be very small, indicating that the bond path, BP, is not curved, and ϵ can present a small value. All these criteria indicate that the BCP will not collapse in the RCP with a small change in geometry. Also, the stabilization energy of a carbon, because of formation of transanular interaction, ΔE(C), can be determined. ΔE(C) is obtained by the difference between the atomic energies of carbon atoms involved in the interactions and the average energy of the other carbons. According to the results reported in Table 6, the BPL is not curved, the differences $r_b - r_r$ and $\rho_b - \rho_r$ are large, and ϵ is small, indicating that the transanular interactions are stable. The evaluated stabilization energies, ΔE(C), show that each interaction gives a stabilizing contribution of 30.0 kcal mol^{-1} to the energies of **2a** and **2b**, respectively, three times larger than the largest energies for H−H bond, as observed by Matta et al.[46]

In addition to the local topological properties at CPs, a set of atomic properties, such as atomic charges $q(\Omega)$, first moment of an atom's charge distribution $M(\Omega)$, atomic volume $v(\Omega)$, and the negative of the total atomic energy $E(\Omega)$, were obtained by the integration over the atomic basins of atoms not related by symmetry. Figure 6 plots the average atomic properties for groups of atoms such as carbons of rings **A** and **B** (Figure 1), carbons of bridges, hydrogens of rings **A** and **B**, and hydrogens of bridges. According to Figure 6a and Table S2 (Supporting Information), the atomic charges are more negative at ring carbons than at bridge carbons. The charges of the carbon atoms increase from **1** to **3**, mainly the charges in the bridge carbons. As a consequence, the atomic charges of hydrogen atoms located at rings or bridges decrease from **1** to **3**. The largest variation

TABLE 7: Bond Critical Points Proprieties (au), Stabilization Energy of C−C Interactions, in kcal mol^{-1}, and $r_b - r_r$, BL, and BPL (au) for the Conformers 2a and 2b (MP2/6-31+G(d,p))

compounds	**CPs**	ρ_b	$\nabla^2\rho_b$	ϵ	G_b	V_b	H_b	$r_b - r_r$	**BL**	**BPL**	ΔE**(C)**
2a	ξ	0.023	0.067	0.043	0.0164	-0.0161	0.0004	1.863	4.934	4.940	30.06
	BCP_{ring}	0.306	−0.817	0.208	0.1063	−0.4169	−0.3106	2.294	2.655	2.655	
2b	ξ	0.020	0.061	0.080	0.0144	−0.0136	0.0009	1.725	5.070	5.082	30.75
	BCP_{ring}	0.306	−0.819	0.204	0.1071	−0.4174	−0.3119	2.294	2.651	2.651	

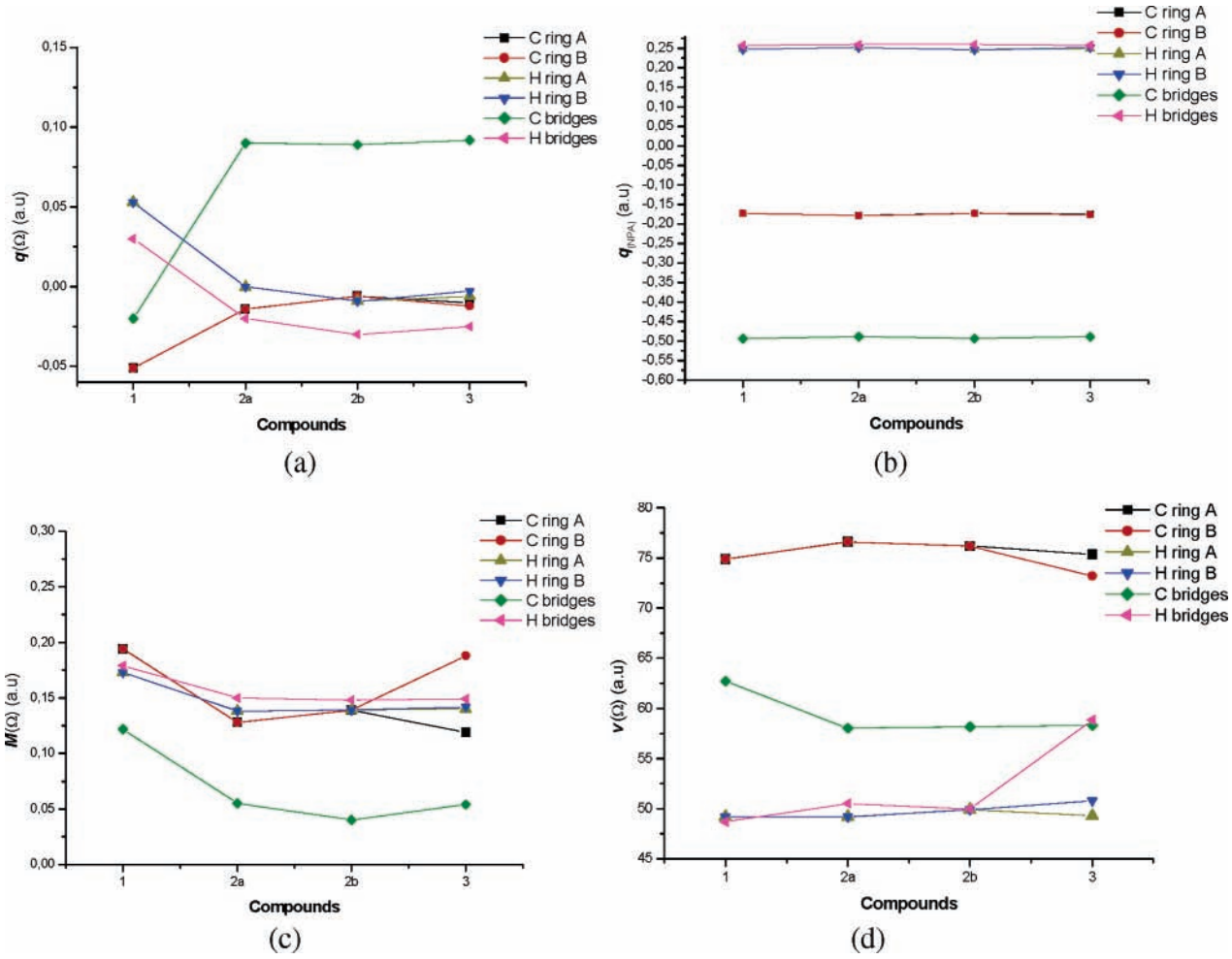

Figure 6. Averaged atomic properties obtained by integration over atomic basin: (a) $q(\Omega)$, (c) $M(\Omega)$, (d) $v(\Omega)$, and the natural atomic charges: (b) q(NPA).

is observed from **1** to **2a**. These results show that the distribution of the atomic charges is not only affected by the changes on the conformation but also by the position of the bridges. When the bridges are located at para position, **1**, carbon atoms present faintly negative charges and hydrogen atoms present slightly positive charges, but when the bridges are located at meta or meta−para positions, the inverse behavior is observed. Comparing the AIM atomic charges with the NBO atomic charges, NPA (natural population analysis), (Figure 6c), it is seen that the NPA charges for carbons belonging to rings or bridges are more negative than the AIM charges, and an opposite behavior is observed in relation to the hydrogen atoms. Therefore, the NPA charges do not follow the AIM pattern. In addition, the NPA atomic charges indicate that there is a preferential charge concentration in the bridge carbons.

The first momentum $M(\Omega)$ arises from the polarization of the individual atomic distributions, describing how the electron density is distorted at a specific atom.[47] According to Figure 6b, $M(\Omega)$ for carbons in ring **B** decreases from **1** to **2a**, and it increases from **2a** to **3**. A different behavior is observed for carbons in ring **A**; a decrease of $M(\Omega)$ is observed from **2b** to **3**. Therefore, carbons of rings that present bridges connected at para position have larger $M(\Omega)$ than carbons of rings with bridges at meta position. In addition, the first moment of bridge carbons is reduced in comparison with ring carbons, indicating a small distortion in the sphericity of the former, which is understandable by the presence of a p_π orbital in the latter. The momentum of hydrogen atoms is similar in all isomers, indicating that the charge distortion is not affected by the position of the bridges. The atomic volumes $v(\Omega)$ are described as a measure of the part of the space enclosed by the intersection of its interatomic surfaces and an envelope of the charge density[48] (in this case 0.001 u.a.). The considered cyclophanes presented large values of $v(\Omega)$ for carbons of rings, in comparison with bridge carbons or hydrogens (Figure 6d). This can be attributed to a diffuse π electron density at this region. In addition, $v(\Omega)$ for bridge carbons decreases form **1** to **2a** and is constant from **2a** to **3**, as observed in atomic charges. In relation to the hydrogens of rings, all compounds exhibited similar atomic volumes, except the hydrogens of **3**. The atomic energies $E(\Omega)$ are very similar for all compounds. For instance, $-E(\Omega)$ for hydrogens is around 0.60 u.a. and for carbons is 38.0 u.a. In this sense, $q(\Omega)$, $M(\Omega)$, and $v(\Omega)$ are either affected by the changes on conformations or influenced by the changes on the bridge position, while $E(\Omega)$ is not changed by any of these factors.

4. Conclusions

An analysis of the electron density, obtained by B3PW91/6-31+G(d,p), B3LYP/6-31+G(d,p), and MP2/6-31+G(d,p) for[2,2] cyclophanes isomers, [2.2]paracyclophane (**1**), *anti*-[2.2]metacyclophane (**2a**), *syn*-[2.2]metacyclophane (**2b**), and [2.2]-metaparacyclophane (**3**), was made by NBO, NSA, and AIM methods and by analysis of frontier molecular orbitals. The NBO analysis not only showed that all isomers present through-bond interactions but also pointed out that only **2a** and **2b** have

through-space interactions, and the RS **1A′** exhibited a very small through-space interaction. On the other hand, NSA results showed that the destabilizing interactions can occur by both mechanisms: through-bond or through-space. Therefore, the [2.2]cyclophanes are mainly stabilized by through-bond interactions. Only the shapes of the frontier MOs of **1**, **2a**, and **2b** suggested the presence of through-space interactions. In close agreement with the NBO and MO analyses, AIM theory pointed out that the through-space interactions of **2a** and **2b** exhibit characteristics of closed-shell interactions. In addition, the properties of BCPs that connect carbons from different rings show that the transannular interactions are stable and that they contribute approximately 30.0 kcal mol^{-1} to the energies of **2a** and **2b**. In addition, the atomic properties computed over the atomic basins showed that the position of the bridges and the relative position of the rings can affect the atomic charges, the first atomic moments, and the atomic volumes. Consequently, according to the considered analyses, all isomers of [2.2]-cyclophanes are stabilized by through-bond interactions, but only the conformers of [2.2]metacyclophane (**2a** and **2b**) present significant through-space stabilizations.

Acknowledgment. The authors acknowledge the Brazilian foundations FAPESP, CAPES, and CNPq for financial support. G.F.C thanks FAPESP for a Ph.D scholarship (Grant 02/03753-5), and S.E.G. thanks CNPq for a research scholarship (Grant 302014/2004-7).

Supporting Information Available: Atomic properties (Table S1) obtained through integrations over atomic basins of the considered [2.2]cyclophanes. This material is available free of charge via the Internet at http://pubs.acs.org.

References and Notes

(1) Schultz, J.; Vögtle, F. *Top. Curr. Chem.* **1994**, *172*, 41.
(2) Boekelheide, V. *Top. Curr. Chem.* **1983**, *113*, 87.
(3) Cram, D. J.; Cram, J. M. *Acc. Chem. Res.* **1971**, *4*, 204 and refs therein.
(4) Wörsdöfer, U.; Vögtle, F.; Nieger, M.; Waletzke, M.; Grimme, S.; Glorius, F.; Pfalts, A. *Synthesis* **2001**, *4*, 597.
(5) Tabushi, I.; Yamamura, K. *Top. Curr. Chem.* **1983**, *113*, 145.
(6) Jones, C. J. *Chem. Soc. Rev.* **1998**, *27*, 289.
(7) Lahann, J.; Höcker, H.; Langer, R. *Angew. Chem., Int. Ed.* **2001**, *40*, 4, 726.
(8) Popova, E.; Antonov, D.; Sergeena, E.; Vonrotsov, E.; Stash, A.; Rozenberg, V.; Hopof, H. *Eur. J. Inorg. Chem.* **1998**, 1733.
(9) Lara, K. O.; Godoy-Alcatar, C.; Rivera, I. L.; Eliseev, A. V.; Yatsimirski, A. K. *J. Phys. Org. Chem.* **2001**, *14*, 453.
(10) Piatnitski, E. L.; Flowers, R. A., II; Deshayes, K. *Chem.—Eur. J.* **2000**, *6*, 999.
(11) Smithrud, D. B.; Wyman, T. B.; Diedrich, F. N. *J. Am. Chem. Soc.* **1991**, *113*, 5420.
(12) Heilbronner, E.; Yang, Z. *Top. Curr. Chem.* **1984**, *115*, 1.
(13) Gerson, F. *Top. Curr. Chem.* **1984**, *115*, 57.
(14) Yamato, T.; Furukawa, T.; Tanaka, K.; Ishi-i, T.; Tashiro, M. *Can. J. Chem.* **2003**, *81*, 244.
(15) Yamato, T.; Okabe, R.; Shigekuni, M.; Furukawa, T. *J. Chem. Res. (S)* **2003**, 608.
(16) Fedyanin, I. V.; Lyssenko, K. A.; Starikova, Z. A.; Antipin, M. Y. *Russ. Chem. Bull., Int. Ed.* **2004**, *53*, 1153.
(17) Zyss, J.; Ledoux, I.; Volkov, S.; Chernyak, V.; Mukamel, S.; Bartholomew, G. P.; Bazan, G. C. *J. Am. Chem. Soc.* **2000**, *122*, 11956.
(18) Bartholomew, G. P.; Ledoux, I.; Mukamel, S.; Bazan, G.; Zyss, J. *J. Am. Chem. Soc.* **2002**, *124*, 13480.
(19) Frontera, A.; Quiñonero, D.; Garau, C.; Costa, A.; Ballester, P.; Deyà, P. M. *J. Phys. Chem. A* **2006**, *110*, 5144.
(20) Quiñonero, D.; Frontera, A.; Garau, C.; Ballester, P.; Costa, A.; Deyà, P. M.; Pichierri, F. *Chem. Phys. Lett.* **2005**, *408*, 59.
(21) Frontera, A.; Quiñonero, D.; Garau, C.; Ballester, P.; Costa, A.; Deyà, P. M.; Pichierri, F. *Chem. Phys. Lett.* **2006**, *417*, 371.
(22) Caramori, G. F.; Galembeck, S. E.; Laali, K. K. *J. Org. Chem.* **2005**, *70*, 3242.
(23) Perdew, J. P.; Burke, K.; Wang, Y. *Phys. Rev. B* **1996**, *54*, 16533.
(24) Petersson, G. A.; Tensfeldt, T. G.; Al-Laham, M. A.; Shirley, W. A.; Mantzaris, J. *J. Chem. Phys.* **1988**, *89*, 2193.
(25) Becke, A. D. *J. Chem. Phys.* **1993**, *98*, 5648.
(26) Frisch, M. J.; Gordon, M. H.; Pople, J. A. *Chem. Phys. Lett*. **1990**, *166*, 275.
(27) Frisch, M. J.; Trucks, G. W.; Schlegel, H. B.; Scuseria, G. E.; Robb, M. A.; Cheeseman, J. R.; Zakrzewski, V. G.; Montgomery, J. A.; Stratmann, R. E.; Burant, J. C.; Dapprich, S.; Millam, J. M.; Daniels, A. D.; Kudin, K. N.; Strain, M. C; Farkas, O.; Tomasi, J.; Barone, V.; Cossi, M.; Cammi, R.; Mennucci, B.; Pomelli, C.; Adamo, C.; Clifford, S.; Ochterski, J.; Petersson, G. A.; Ayala, P. Y.; Cui, Q.; Morokuma, K.; Malick, D. K.; Rabuck, A. D.; Raghavachari, K.; Foresman, J. B.; Cioslowski, J.; Ortiz, J. V.; Stefanov, B. B.; Liu, G.; Liashenko, A.; Piskorz, P.; Komaromi, I.; Gomperts, R.; Martin, R. L.; Fox, D. J.; Keith, T.; Al-Laham, M. A.; Peng, C. Y.; Nanayakkara, A.; Gonzalez, C.; Challacombe, M.; Gill, P. M. W.; Johnson, B. G.; Chen, W.; Wong, M. W.; Andres, J. L.; Head-Gordon, M.; Replogle, E. S.; Pople, J. A. *Gaussian 98*, Revision A.7; Gaussian, Inc.: Pittsburgh, PA, 1998.
(28) Carpenter, J. E.; Weinhold, F. *J. Mol. Struct.* **1988**, *169*, 41.
(29) Badenhoop, J. K.; Weinhold, F. *J. Chem. Phys.* **1997**, *107*, 5406.
(30) Bader, R. F. W. *Atoms and Molecules- A Quantum Theory*; Claredon Press: Oxford, New York, 1994.
(31) (a) Glendening, E. D.; Weinhold, F. *J. Comput. Chem.* **1998**, *19*, 593. (b) Glendening, E. D.; Weinhold, F. *J. Comput. Chem.* **1998**, *19*, 610. (c) Glendening, E. D.; Badenhoop, J. K.; Weinhold, F. *J. Comput. Chem.* **1998**, *19*, 628.
(32) Glendening, E. D; Badenhoop, J. K.; Reed, A. E.; Carpenter, J. E.; Bohmann, J. A.; Morales, C. M.; Weinhold, F. *NBO 5.0;* Theoretical Chemistry Institute, University of Wisconsin: Madison, WI, 2001.
(33) Popelier, P. L. A.; Bone, R. G. A. *MORPHY98*; UMIST: Manchester, U.K., 1998.
(34) Biegler-Konig, F.; Schonbohm, J.; Bayles, D. *J. Comput. Chem.* **2001**, *22*, 545.
(35) Portmann, S.; Lüthi, H. P. MOLEKEL, An Interactive Molecular Graphics Tool. *Chimia* **2000**, *54*, 766.
(36) Wendt, M.; Weinhold, F. *NBOView 1.0, NBO Orbital Graphics*; Department of Chemistry, University of Wisconsin: Madison, WI, 2001.
(37) Henseler, D.; Hohlneicher, G. *J. Phys. Chem. A* **1998**, *102*, 10828.
(38) Rauk, A. *Orbital Interaction Theory of Organic Chemistry*; John Wiley & Sons, INC: New York, 1994.
(39) Salcedo, R; Mireles, N; Sansores, L. E. *J. Theor. Comp. Chem.* **2003**, *2* (2), 171.
(40) Lyssenko, K. A.; Antipin, M. Y.; Antonov, D. Y. *ChemPhysChem.* **2003**, *4*, 817.
(41) (a) Haaland, A.; Shorokhov, D. J.; Tverdova, N. V. *Chem.—Eur. J.* **2004**, *10*, 4416. (b) Poater, J.; Solà, M.; Bickelhaupt, M. F. *Chem.—Eur. J.* **2006**, *12*, 2889.
(42) (a) Bader, R. F. W. *J. Phys. Chem. A* **1998**, *102*, 7314. (b) Bader, R. F. W. *Chem.—Eur. J.* **2006**, *12*, 2896.
(43) Bader, R. F. W.; Essén, H. *J. Chem. Phys.* **1984**, *80*, 1943. (b) Koritsanszky, T. S.; Coppens, P. *Chem. Rev.* **2001**, *101*, 1583.
(44) Cremer, D.; Kraka, E. *Angew. Chem., Int. Ed. Engl.* **1984**, *23*, 627.
(45) Bader, R. F. W. *J. Chem. Phys.* **1980**, *73*, 2871.
(46) Matta, C. F.; Trujillo, J. H.; Tang, T. H.; Bader, R. F. W. *Chem.—Eur. J.* **2003**, *9*, 1940.
(47) Bader, R. F. W.; Larouche, A.; Gatti, C.; Carrol, M. T.; MacDougall, P. J.; Wiberg, K. B. *J. Chem. Phys.* **1987**, *87*, 1142.
(48) Bader, R. F. W.; Carrol, M. T.; Chesseman, J. R.; Chang, C. *J. Am. Chem. Soc.* **1987**, *109*, 7968.